RAPID COMMUNICATIONS

PHYSICAL REVIEW B VOLUME 46, NUMBER 19 15 NOVEMBER 1992-I

Inelastic x-ray scattering in single-crystal C_{60}

E. D. Isaacs and P. M. Platzman
AT&T Bell Laboratories, 600 Mountain Avenue, Murrary Hill, New Jersey 07974

P. Zschack
Oak Ridge National Laboratory at the National Synchrotron Light Source, Beamline X14, Brookhaven National Laboratory, Upton, New York 11973

K. Hamalainen
National Synchrotron Light Source, Brookhaven National Laboratory, Upton, New York 11973

A. R. Kortan
AT&T Bell Laboratories, 600 Mountain Avenue, Murray Hill, New Jersey 07974
(Received 20 July 1992)

We have measured energy-loss spectra of electrons in a single crystal of C_{60} for several momentum transfers ($0.65 \leq q \leq 1.15$ Å^{-1}) with energy resolution of 1.5 eV by the inelastic scattering of synchrotron x rays. Two features dominate the spectra; an interband transition near 5 eV due to the carbon $2p_z$ electrons, and a bulk plasmon mode peaked near 30 eV, which arises from all four of the carbon valence electrons. The spectra are isotropic.

An understanding of the electronic structure in undoped C_{60} crystals is essential for an understanding of the effects of electron doping and the nature of complex states such as superconductivity and magnetism. Recently, there have been a number of measurements of the electronic excitation spectrum in undoped C_{60}. However, techniques such as photoionization are limited to surfaces or gases of C_{60} molecules, and are difficult to interpret.[1] High-energy electron-energy-loss spectroscopy (EELS) experiments are limited to small momentum transfers or very thin samples because of multiple scattering and are very sensitive to surface effects.[2–5] The most suitable technique currently available to probe electronic structure in the 1-eV energy resolution region is inelastic x-ray scattering spectroscopy (IXSS).[6] The weak interaction between x rays and the electronic system greatly reduces multiple scattering, which in principle allows IXSS to probe the bulk system over a broad range of momentum transfers. The availability of bright synchrotron x-ray sources in fact allows us to perform such experiments.

We present IXSS measurements in a single crystal of C_{60} with an energy resolution of 1.5 eV. These measurements have been made for several momentum transfers along the [001] and [111] crystal axes with an incident energy $\hbar\omega = 5.66$ keV. We observe two spectral features. At an energy loss near 5 eV there is a sharp interbandlike feature for momentum transfer $q = 0.65$ Å^{-1}, which disperses to 6.5 eV at $q = 1.15$ Å^{-1}. At an energy loss of 27 eV there is a broad bulk plasmonlike mode for momentum transfer $q = 0.65$ Å^{-1}, which disperses to 30.3 eV for $q = 1.15$ Å^{-1}. Finally, the integrated intensity of the bulk plasmon mode grows by a factor of 5 over this momentum range while the intensity of the smaller, low-energy peak remains unchanged. These spectra will be compared to those for a gas of C_{60} molecules taken with EELS, and to those for graphite taken with IXSS.

The measurements of the energy-loss function, $S(\mathbf{q},\omega)$, reported here, were carried out at the dipole magnet beamline X14 and at the wiggler beamline X25. The energy of the incident beam was tuned to 5.66 keV with a full width at half maximum (FWHM) of approximately 1 eV at X14 and 0.7 eV at X25 as determined by double-crystal monochromators and collimating slits. The single-crystal C_{60} sample size was approximately $0.2 \times 0.3 \times 0.5$ mm^3 with glossy, black [001] and [111] facets that were both normal to the 0.5-mm sample face. A mosaic spread of 0.02 degrees attested to the high quality of the crystal. The experiments were carried out at room temperature with the sample mounted in vacuum on a tungsten pin with the [001] and [111] axes both normal to the pin. With this configuration, both axes could easily be rotated into the scattering vector $\mathbf{q}$.

Single crystal C_{60} is favorable for IXSS studies because the relatively low x-ray absorption of carbon allows a large sample volume for scattering. The x-ray absorption length in single crystal C_{60} is approximately 0.5 mm at 5.66 keV. X-ray absorption has limited IXSS studies to materials lighter than silicon ($Z = 14$). However, this is expected to change with the availability of brighter sources, such as the insertion device X21 at the National Synchrotron Light Source and future machines such as the ESRF and APS. Unfortunately, even with low absorption in carbon, long counting times were necessary because in general IXSS cross sections are small. In addition, the x-ray beam spot size was approximately 1×1 mm^2, which is considerably larger than our sample. For example, a counting time of about 160 min was necessary to obtain a single spectrum at $q = 1.15$ Å^{-1} with better than 2% statistics in the plasmon peak (see Fig. 1).

The scattered radiation was collected by a cylindrically

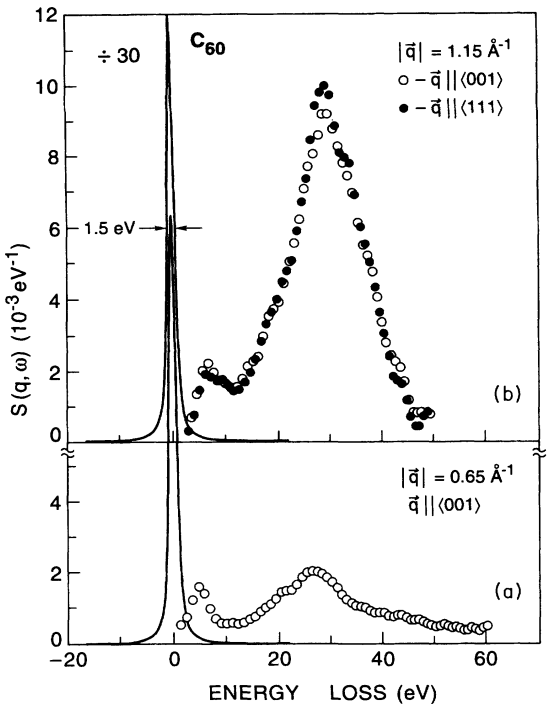

FIG. 1. (a) $S(\mathbf{q},\omega)$ for a single crystal of C_{60} for $q = 0.65$ Å^{-1} and parallel to the [100] axis. The elastic peak is shown divided by a factor of 30. The energy resolution, as described in the text, is 1.5 eV. (b) $S(\mathbf{q},\omega)$ for a single crystal of C_{60} for $q = 1.15$ Å^{-1}, for q parallel to the [100] (open circles) and [111] (filled circles) crystal axes, respectively. The scans are very similar within our experimental uncertainty.

bent, 5 cm axial×7.5 cm tangential, highly oriented pyrolytic graphite mosaic (0.4°) crystal analyzer, bent to a 500-mm radius-of-curvature by Union Carbide. The cylindrical (flat) axis was in the vertical scattering plane and was chosen as the dispersive direction. The analyzer was placed equidistant (500 mm) from the sample and a 10-cm-long position-sensitive proportional counter. This configuration gave a one-to-one para-focusing of the source onto the detector with a total bandpass of 80 eV. In this way the entire energy-loss spectrum was obtained simultaneously.[7]

The response function of the analyzer-detector combination was determined by scanning the beamline monochromator energy while measuring the intensity of the elastic peak on the wire detector for a fixed analyzer angle. The spectra presented below have been divided by this measured response. The energy resolution as given by the FWHM of the elastic peak (see Fig. 1) was measured to be 1.5 eV. It should be noted that the angular spread of the elastic peak, and hence energy resolution at the wire, is a function of energy, i.e., from Braggs law $\Delta\theta = (\Delta\omega/\omega)\tan\theta$, where $\Delta\omega$ is fixed by the monochromator. However, since all of the spectral features were considerably broader than the instrumental resolution, particularly at large energy transfer (smaller energy photons) no deconvolution was necessary. Finally, the spatial resolution of the wire was 50 μm, which at the high-angle side (larger energy transfer and nearer backscattering) of the wire corresponded to an energy spread of about 100 meV. Therefore, the wire oversampled the data by at least a factor of 15, allowing us to integrate flux over 250 μm (0.5 eV) of detector wire without degrading the energy resolution. This was accomplished with a multichannel analyzer which measured the output signal of the detector.

The experimental data were processed in two ways. First, the elastic line was removed by fitting it to a symmetric function. The fit is shown in the figure reduced by a factor of 30. Due to the high intensity of the elastic line the data in the 0–4-eV energy-loss range was somewhat less reliable. As such, the line shape of the low-energy spectral peak was somewhat uncertain, while the peak position was better determined. Second, all of the spectra were normalized via the f-sum rule, $\int_0^\infty S(\mathbf{q},\omega)\omega\, d\omega = \hbar q^2/2m$. Errors in the normalization were due to the presence of scattering from the core electrons (i.e., $2p$ and $1s$). These were less than 10% since most of that scattering was at higher energy loss with a sharp onset at 72.5 eV (L_{III} edge), and only exponential tails extended to lower energy loss.

The energy-loss spectrum for $q = 0.64$ Å^{-1}, with $\mathbf{q}$ along the [001] crystal axis, is shown in Fig. 1(a). The spectrum shows two distinct peaks; one at 4.9 eV with a FWHM of 3 eV, and a second peak at 27 eV with a FWHM of 14.7 eV. In addition, there is evidence for a shoulder on the low-energy side of the second peak, near 20 eV. In Fig. 1(b) two sets of data are shown for $q = 1.15$ Å^{-1} with the momentum transfer along both the [001] and [111] crystal axes, respectively. The spectra are similar, i.e., there is no evidence for anisotropy. It should also be noted that both of these IXSS spectra are very similar to the spectra in a crystalline powder of C_{60} obtained by us previously. The spectrum itself shows that the lower-energy peak shifts to 6.5 eV while the broad peak shifts to 30.3 eV. A shoulder on the high-energy peak is still present. In addition, while the integrated intensity of the low-energy transition remains nearly unchanged, that of the broad peak grows by a factor of 5. Finally, the width of the 4.9-eV peak broadens from 3 to 4 eV, while the 27-eV peak broadens from 14.6 to 15.4 eV.

Comparison of our IXSS measurements in the solid with intermediate energy (1 keV) EELS in a gas of C_{60} molecules reveals a number of differences. The dominant low-energy feature in the molecule is observed at 6 eV with $q = 0.42$ Å^{-1}, while there is a weaker peak at 4.9 eV, where we observe the low-energy peak in the solid. Though the IXSS experiment does not have good enough energy resolution to observe this fine structure, we suggest that it is possible that the intermolecular overlap in the solid could wash out the fine structure.

At higher energies in the molecule there is a broad feature which is centered near an energy loss of 22 eV and has a multiple bump structure. This is in contrast to the single peak seen in the solid near 30 eV. It has been

suggested by the authors that the structure might be attributed to the high degree of symmetry of the C_{60} molecule, i.e., band structure on the molecule. Finally, the relative scattering intensities of the two principal peaks in the molecule is reversed, with the low-energy peak being considerably stronger.

IXSS measurements in graphite with the momentum transfer in the a-b plane show two spectral features which are remarkably similar to the single-crystal C_{60} spectra.[6] There is a spectral peak at 8 eV with a FWHM of about 3 eV which does not disperse for intermediate momentum transfers. There is also a feature peaked near 30 eV, whose width is about 15 eV. In addition, the ratio of intensities of the high-energy to low-energy peaks grows with momentum transfer in much the same way as in the C_{60} solid.

The inelastic x-ray scattering cross section is a direct measure of the electronic excitation spectrum, i.e., the dynamic structure factor, $S(\mathbf{q},\omega)$;

$$\frac{d\sigma}{d\Omega\, d\omega}=(\mathbf{e}_1\cdot\mathbf{e}_0)^2\left[\frac{\omega_1}{\omega_0}\right]r_0^2 S(\mathbf{q},\omega) \tag{1}$$

and

$$S(\mathbf{q},\omega)=\frac{q^2}{4\pi e^2}\mathrm{Im}[\epsilon^{-1}(\mathbf{q},\omega)]\ , \tag{2}$$

where $\mathbf{q}=(\mathbf{q}_1-\mathbf{q}_0)$ and $\omega=(\omega_1-\omega_0)$ are the momentum and energy transferred during the scattering process and $(\mathbf{q}_0,\omega_0)$ and $(\mathbf{q}_1,\omega_1)$ are the momentum and energy of the incident and scattered radiation, respectively. The complex dielectric function $\epsilon(\mathbf{q},\omega)$ is a matrix in band indices, $(\mathbf{e}_0,\mathbf{e}_1)$ are the polarization of the incident and scattered radiation, and r_0 is the classical electron radius. At low momentum transfers, in a free-electron metal such as aluminum (i.e., jellium), $S(\mathbf{q},\omega)$ is dominated by the plasmon with a small contribution from a single-particle state at small ω.[8] Though band-structure effects are unimportant in jellium, the structure of $S(\mathbf{q},\omega)$ is significantly complicated by electron correlation effects, which broaden the plasmon at small q and gives rise to structure in the single-particle peak at intermediate q.[9,10] On the other hand, in semimetals and insulators, such as graphite or single-crystal C_{60}, band-structure effects on $S(\mathbf{q},\omega)$ become important. At small q, these band-structure effects appear as dipole interband transitions, as in the optical spectra, which occur in the eV energy-loss region of the spectrum. At larger ω one expects a plasmon excitation, which can be modified by the presence of band structure. For example, this can be seen in the anisotropic spectra of graphite or lithium.[6,11]

Attempts to model the electronic structure in C_{60} have been limited to the isolated molecule. These models have taken the two extreme approaches of either the electron liquid (jellium) or the band-structure model. For example, Barton and Eberlein treat a molecule of C_{60} as jellium consisting of two electron fluids that support multipole plasmons and include simple screening via a static dielectric function.[12] On the other hand, the tight-binding approximation has been applied by Bertsch *et al.* where the C_{60} molecule is treated as a collection of isolated atoms.[13] While both of these models were analyzed in the random-phase approximation (RPA), they were reasonably successful in describing the general features of the low-energy peak that is observed by us and in the molecular gas. Unfortunately, since these theories do not include solid-state effects they are unsuccessful in describing the high-energy region of the spectrum in our data.

In molecular C_{60} the carbon $2p_z$ orbitals project normal to the surface. In graphite, these orbitals form the π bonding and π^* antibonding states. The peak at 4.9 eV in the solid is consistent with the energy expected for dipole-allowed interband transitions between the π and π^* states. The similarity of this feature with that observed in the molecule strongly suggests that it is localized on the molecule. The dispersion and slight broadening of the π transition between $q=0.65$ and 1.15 Å^{-1} is consistent with the itinerant nature of the π electrons on the molecule, i.e., π bands. However, it will be interesting to determine what the intermolecular effects on these π bands are, by probing with IXSS at $q<2\pi/R_{C_{60}}\cong 0.6$ Å^{-1}, where the distance scales probed are larger than the size of a single C_{60} molecule, $R_{C_{60}}$.

A preliminary understanding of the high-energy excitation can be attained by considering the RPA plasmon dispersion which is given by

$$\omega(q)\cong\omega_p\left\{1+\frac{3}{5}\left[\frac{qv_F}{\omega_p}\right]\right\}^2\ , \tag{3}$$

where $\omega_p=\sqrt{4\pi ne^2/m}=21.5$ eV. The electron density is $n=3.35\times10^{23}/\text{cm}^3$, which assumes that all four of the carbon valence electrons ($2s$, $2p_x$, $2p_y$, and $2p_z$) contribute. The Fermi velocity is $v_F=2.49\times10^8$ cm/sec. From Eq. (3) the plasmon energy at $q=0.65$ Å^{-1} is expected at approximately 23.1 eV while at $q=1.15$ Å^{-1} it is expected at 26.5 eV. Although this amount of dispersion is consistent with our measurements, the absolute value of the plasmon energy does not agree. The disagreement is probably due to the pushing up of the plasmon energy by electronic interband transitions. A similar effect can be seen in graphite, where the observed plasmon energy is clearly shifted up in energy from the RPA value of 25 eV and is very anisotropic.[6,11] In diamond the plasmon energy is observed very close to its RPA value at 31 eV. The exceptionally high plasmon energy in diamond decouples the plasmon from the effects of band structure at lower energies.

We have presented IXSS measurements in a bulk single crystal of C_{60}. The lower-energy peak in the spectra of the solid is similar to a gas of C_{60} molecules demonstrating the local nature of this interband mode. The high-energy plasma oscillation, which arises from the four carbon valence electrons is quite different from the molecule. This is primarily due to the higher bulk electronic density in the solid. The additional 4-eV discrepancy with RPA is most likely due to band-structure effects on the plasmon, similar to what is observed in graphite. Finally, it will be interesting to determine the effects on $S(\mathbf{q},\omega)$ of doping single-crystal C_{60} into the superconducting regime. In general, the effects are expected to be at energies below the interband transition at 5 eV, since the

plasmon energy for the relatively low doping concentration is in the 1-eV range. Since we have demonstrated the isotropy of the IXSS (in the $q = 1$ A^{-1} range) in a single crystal, it will be possible to study a powder of C_{60} crystallites, where doping is possible.

We thank Hugh Williams for his extensive assistance in data analysis. We also acknowledge Lonnie Berman, Robert Flemming, Jerry Hastings, Mitch Nelson, and Michael Schluter for enlightening conversations and George Wright for his expert technical assistance. Oak Ridge National Laboratory beamline X14 is supported in part by the Division of Materials Sciences and Division of Chemical Sciences, U.S. Department of Energy under Contract No. DE-AC05-840R21400 with the Martin Marietta Energy Systems, Inc.

[1]I. V. Hertel *et al.*, Phys. Rev. Lett. **68**, 784 (1992).
[2]G. Gensterblum *et al.*, Phys. Rev. Lett. **67**, 2171 (1991).
[3]J. W. Keller and M. A. Coplan (unpublished).
[4]Y. Saito, J. Shinohara, and A. Ohshita, Jpn. J. Appl. Phys. **30**, L1068 (1991).
[5]H. Cohen *et al.*, Solid State Commun. **81**, 183 (1992).
[6]W. Schulke, U. Bonse, H. Nagasawa, A. Kaprolat, and A. Berthold, Phys. Rev. B **38**, 2112 (1988).
[7]G. E. Ice and C. J. Sparks, Nucl. Instrum. Methods A **291**, 110 (1990); E. D. Isaacs, P. Zschack, P. M. Platzman, G. E. Ice, and D. W. Berreman (unpublished).
[8]D. Pines and P. Nozieres, *The Theory of Quantum Liquids* (Benjamin, New York, 1966).
[9]P. M. Platzman and P. Eisenberger, Phys. Rev. Lett. **33**, 152 (1974).
[10]P. M. Platzman, E. D. Isaacs, H. Williams, P. Zschack, and G. E. Ice (unpublished).
[11]P. M. Platzman and P. Eisenberger, Phys. Rev. B **13**, 934 (1976).
[12]G. Barton and C. Eberlein, J. Chem. Phys. **95**, 1512 (1991).
[13]G. F. Bertsch, A. Bulgac, D. Tomanek, and T. Wang, Phys. Rev. Lett. **67**, 2690 (1991).